ISSN 1330-3651 (Print), ISSN 1848-6339 (Online) https://doi.org/10.17559/TV-20240212001324
Original scientific paper

A Study of the Effect of Graphene on Fatigue Life of CuAlNi Shape Memory Alloy

Wasiu Ayinde ISSA*, Hüseyin ÇAMUR, Mahmut SAVAŞ

Abstract: CuAlNi shape memory alloys (SMA) are commonly used in high temperature engineering applications due to their cost-effectiveness and ease of production, as compared to Nickel-Titanium alloys. However, these alloys generally exhibit poor fatigue properties when subjected to cyclic stress. To address this issue, researchers investigated the effect of adding high-purity graphene (C) nanoplatelets on the fatigue life and hardness of CuAlNiSMA. The study found that as the number of stress cycles increased, the stress leading to fatigue failure decreased. Using Design Expert Software version 13.0, current researchers predicted the interaction between fatigue life and the percentage composition of Cu and graphene (C). A novel mathematical model is therefore developed for fatigue life. The model showed a good fit with an R^2 of 0.9487, indicating that it can be employed in fatigue life studies of SMAs containing additions like graphene.

Keywords: CuAlNi; CuAlNiC; fatigue life; mechanical properties; shape memory alloy

1 INTRODUCTION

SMA, short for Shape Memory Alloys, possess the unique characteristic of being able to recover their original shape after being deformed [1], owing to a reversible solid phase transformation [2-7]. This property is exhibited by various alloys such as Ni-Ti, Cu-Zn-Al, and Cu-Al-Ni [1], where a transition between two phases, i.e., martensite at a lower temperature and austenite at a higher temperature, takes place [8-9]. Due to their many intriguing properties [11], including their stability at high temperatures over 100 °C [12], ease of production and low cost [13-15], and electrical and thermal conductivity properties [16], as well as their numerous applications in engineering and other fields [17], research on Cu-based shape memory alloys has recently increased [10]. As a cheaper alternative to the widely used and more expensive NiTi-based SMA alloy [18], CuAlNiSMA is fragile [19], brittle, and not well suited for cyclic activities [20]. Their commercial use is being curtailed in the light of these flaws [21-23]. The objectives of this study includes the following:

1. Determination of the mechanical properties i.e. hardness of the CuAlNi SMA.
2. Improving the mechanical properties of the CuAlNi SMA with fourth element addition i.e. graphene to produce CuAlNiC.
3. Characterizing the microstructure of the CuAlNi and CuAlNiC SMA.
4. Investigating the fatigue behaviour of the CuAlNi and CuAlNiC SMA.
5. Comparison of the fatigue behaviour of the CuAlNi and CuAlNiC SMA.

According to the data reported in the literature, the properties of CuAlNiSM. As can be enhanced through grain refinement [24] and the addition of other elements [18, 25]. Karaduman and Canbay [18] found that the addition of 5 nm graphene nanoplatelets can effectively control the properties of the alloy. Similarly, Saud et al. [26] observed an improvement in the alloy properties by adding trace amounts of carbon nanotubes. However, there is a lack of literature on the impact of graphene addition on the stress-number of cycles curve (fatigue life) of CuAlNiSMA, which is crucial given the cyclic load that the alloy typically experiences [27]. Fatigue failure occurs when materials become increasingly vulnerable to fluctuating stresses, resulting in their resistance decreasing over time [28, 29]. To conduct a fatigue test, a machined component or sample is subjected to known reversal stresses that may or may not be of equal magnitude [30]. This process helps to determine the maximum amount of stress a material or component can withstand before failing in service [1]. The term "hardness" can be used to describe different characteristics of a material, including its ability to withstand cutting, abrasion, scratching, or shaping. Various methods are used to test hardness, such as Brinell, Vickers Microhardness, Knoop Microhardness, Rockwell, and Superficial Rockwell Hardness techniques [31]. To address the challenges associated with extensive experiments and cost reduction, the implementation of artificial intelligence (AI) models can be utilized to forecast the associations between parameters. In order to simulate and predict the fatigue life of Cu-Al-Ni shape memory alloys, computer software programs can be employed. These AI models, also known as phenomenological models, have the capability to provide a more comprehensive and dependable understanding of the intricacies of material fatigue behaviour, as they are based on accurate equations and relationships. This allows for the optimal design of materials.

2 MATERIALS AND METHODOLOGY

2.1 Materials

Copper, aluminium, nickel from Nigeria were procured, weighing 2.5 kg, 1.2 kg, and 0.6 kg, respectively. Additionally, graphene nanoplatelets were obtained from Nanografi Nanotechnology Company, Turkey. These nanoplatelets are quoted to have a size of 5 nm, 99.9% purity and a diameter of 30 μm. The materials are shown in Fig. 1. Cu - 76.444, Al - 12.935, Ni - 4.382 by concentration in the SMA with Si, S, Ca and other earthly materials present in traced quantities due to casting, established the purity of Cu, Al and Ni used.

2.2 Methodology

The casting method was used to prepare the alloy. To begin with, nickel was charged into the furnace due to its high melting point, followed by the addition of copper at

1400 °C. Once the temperature was reached, aluminium was added to the mix.

(a) Graphene nanoplatelets (b) Copper

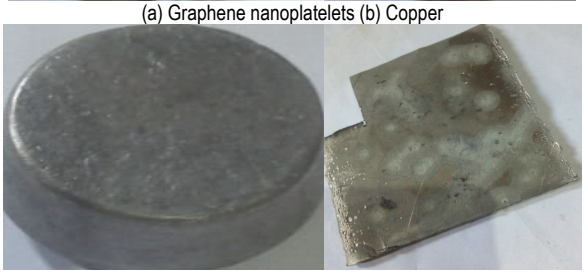

(c) Aluminium (d) Nickel

Figure 1 Materials used

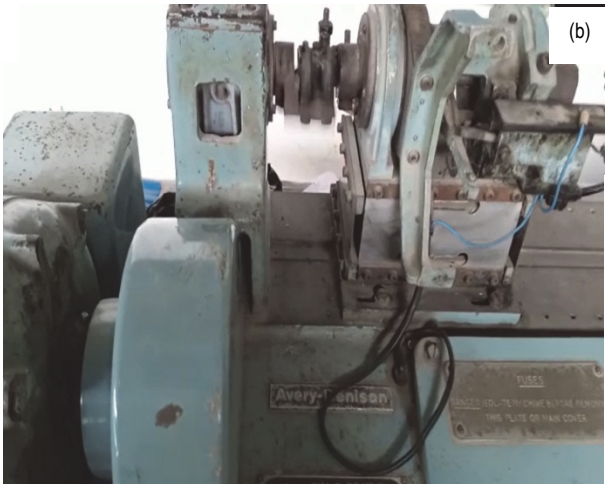

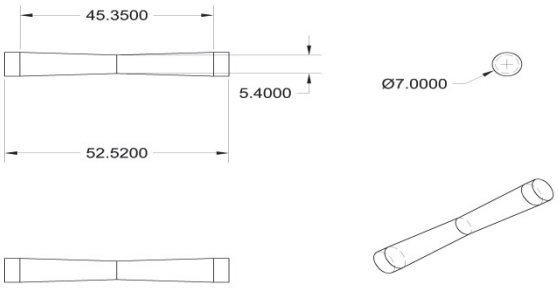

Figure 3 (a) Avery Denison Fatigue Testing Machine, (b) specimen specifications (Gauge length = 45.35 m, Final length = 52.52 m)

The fatigue test is designed to apply reversed load. Grips were provided for both bending and torsion test on flat specimen. The pure bending test we are interested in, the load was imposed at one end of the specimen by an oscillating spindle driven by means of a connecting rod. Crank and eccentrics with the load applied in form of bending moments. The eccentric was mounted directly on a shaft of the electric motor and can be easily adjusted to give the range of bending angles. The number of cycles to failure was determined using a revolution counter, and the values were recorded in Tab. 3. The machine stopped operating once the specimen got fractured. The measured bending moments (from the fatigue test), helps to estimate the applied stress from the relations below [30].

$$\sigma = \frac{M_{\max}}{W} \tag{1}$$

where: σ = Stress, $M_{\max}$ = Machine Measured Bending Moment Value /Kgfcm.

The ingot was stirred to ensure that the alloy was homogeneous. Argon gas was used to shield the atmospheric air to prevent oxidation. The ingot was then air cooled and divided into four samples, A, B, C, and D as shown in Fig. 2. Sample A was used as a control sample, while samples B, C, and D had different percentages of graphene added after heating to 1400 °C.

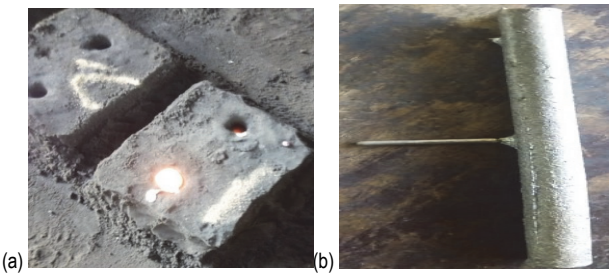

Figure 2 Alloy casting (a) Mould (b) Cast Alloy

$$W = Modulus = \frac{\pi d^3}{32} \tag{2}$$

Stair case method was deployed to apply the bending moment [30]. By this method, the bending moment was applied and then increased with a fixed amount. This serves as the bending moment test value for the succeeding specimen (sample).

3 RESULTS AND DISCUSSION

Four specimen standards of machine specifications were created from each of the samples A, B, C, and D. The compositions of each of the samples are as shown in Tab. 1. The load, in the form of a bending moment, was measured by an oscillating spindle at one end of the specimen. The bending moment was applied with the help of a connecting rod, eccentrics, and crank. The number of cycles to failure for fatigue failure to occur was determined using a revolution. The fatigue testing machine stopped operating once the specimen got fractured. Scanning Electron Microscope (SEM) was used to study the surface morphologies of the samples and Energy Dispersive X-ray

Spectroscope (EDS) to study the elemental compositions of the samples. The results obtained are as shown in Fig. 6 to Fig. 9. The Rockwell Hardness Testing machine with a diamond Indenter Kgf 150 was used to measure the hardness value of samples A, B, C and D. The results obtained are as shown in Tab. 3 and Fig. 5.

3.1 Alloy Composition/Production

The SMA produced from this research has composition as shown in Tab. 1. This is in conformity with those produced from literature containing a fourth element, Tab. 2. The fourth elements added to CuAlNiSMA were added in traced quantities. The mixture was mixed through a continuous stirring to achieve homogenous mixture [13].

Table 1 Percentage Composition of SMA produced

Sample	C / %	Copper / %	Aluminum / %	Nickel / %
A	-	84.3	11.9	3.8
B	0.15	84.78	11.25	3.8
C	0.3	84.05	11.32	3.79
D	0.45	83.92	11.85	3.78

Table 2 Percentage Composition of SMA Produced from literatures [13]

C / %	Co / %	Ti / %	Mn / %	Copper / %	Aluminum / %	Nickel / %
-	-	-	-	84	11.9	4.10
-	-	-	0.97	82.94	11.93	4.16
-	-	0.99	-	82.92	11.94	4.15
-	1.14	-	-	82.96	11.9	4
0.55	-	-	-	84.78	11.25	3.8

3.2 Fatigue Properties

The results presented in Fig. 4 show the fatigue life. The effect of graphene on the fatigue behaviour of CuAlNi SMA is described. It is shown that graphene addition to CuAlNi SMA improves the fatigue life of the alloy. The optimum amount for best fatigue life was observed at 0.3% graphene addition. Other researchers who studied the effect of fourth element addition to CuAlNi SMA added beryllium (Be) and observed that the addition of Beryllium (Be) to Cu-Al-Ni Shape Memory Alloy actually increased the fatigue life [32, 33]. The fatigue life of a material refers to its ability to withstand stress for a certain number of cycles before experiencing a particular type of failure. This is depicted through a graph that shows the relationship between stress (S) and the number of cycles (N) before fatigue fracture occurs. By plotting the stress values against the corresponding number of cycles until the material fails, we can generate an S-N Curve (as shown in Fig. 4).

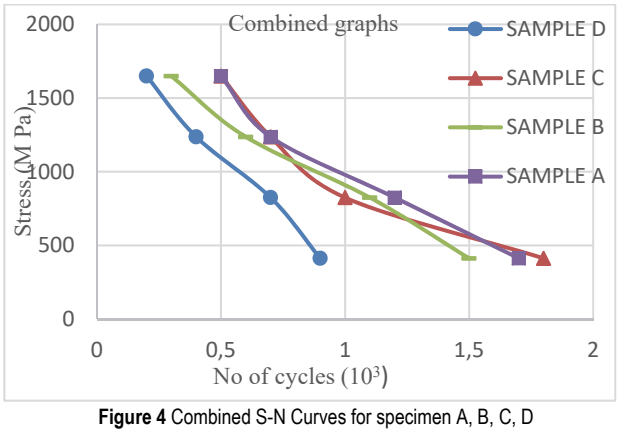

Figure 4 Combined S-N Curves for specimen A, B, C, D

The S-N curves (Fig. 4) demonstrate that as the number of stress cycles increases, the stress level leading to fatigue failure decreases. This is in conformity with theory. The graphs also reveal that samples B and D have fewer stress cycles compared to samples A and C for a given stress value. When the stress value is increased to 1649.25 MPa, sample C has a higher fatigue life than samples A, B, and D. Sample D has a significantly lower fatigue life than samples A, B, and C due to an increase in graphene content. It appears that the sample C with 0.3% graphene at a stress value of 1649.25 MPa represents the optimum.

3.3 Hardness Properties

The effect of graphene on the mechanical property of CuAlNi SMA was investigated through the use of Rockwell hardness testing machine, Tab. 4. The results from the test carried out on samples A (SMA 100%,), B (SMA 99.85%, C 0.15%), C (SMA 99.70%, C 0.3%), B (SMA 99.55%, C 0.45%), show an increase in the hardness value which correspond to an increase in the mechanical property of the alloy. Other researchers carried out vicker's microhardness test on CuAlNi SMA with the addition of fourth element to the alloy such as Mn, Co and Ti. The microhardness value they obtained shows an increase in hardness value with the addition and they attribute this improvement in alloy mechanical property to the presence of precipitates of the added alloying elements to the microstructure of CuAlNi SMA [35, 36].

Table 3 Result of Rockwell Hardness test using a diamond indenter with a scale HRV force 150 Kgf.

Specimen	Test 1	Test 2	Test 3	Average
A	26.0	43.0	29.0	32.7
B	42.0	43.5	46.5	44.0
C	38.5	44.5	42.0	41.8
D	40.0	40.0	41.0	40.5

The Rockwell hardness test showed that samples B, C, and D have higher hardness values compared to sample A without graphene.

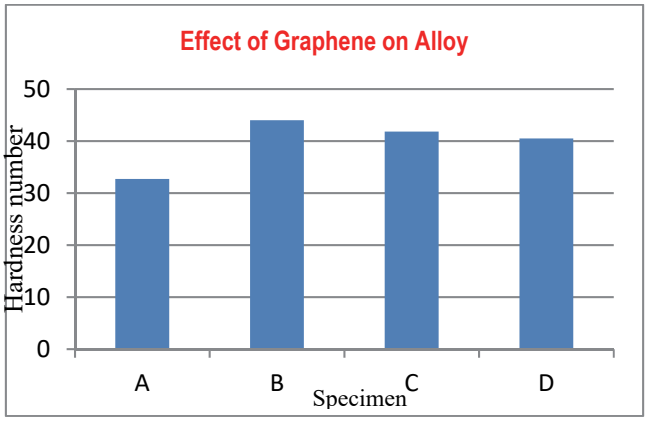

Figure 5 Effect of Graphene on SMA from the results of the hardness test

3.4 Surface Structure/Morphology and Elemental Composition of Samples

3.4.1 Crystal Orientation of the Samples

Fig. 6 presents the Scanning Electron Microscope (SEM) micrograph of sample A (control sample) without

addition of graphene. It is clear from the micrograph that the alloy has a structure appearing in the form of different rock debris lined over another to assume an undulating like layers.

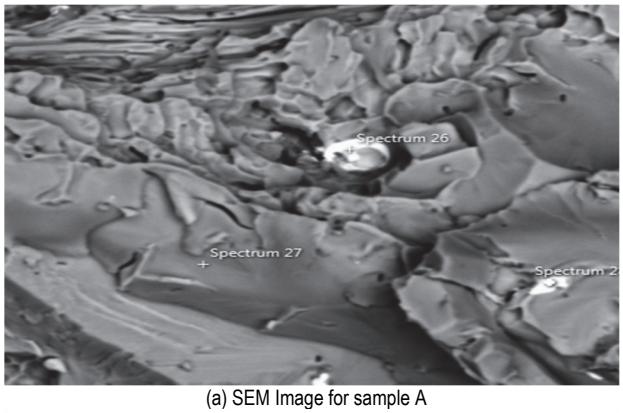

(a) SEM Image for sample A

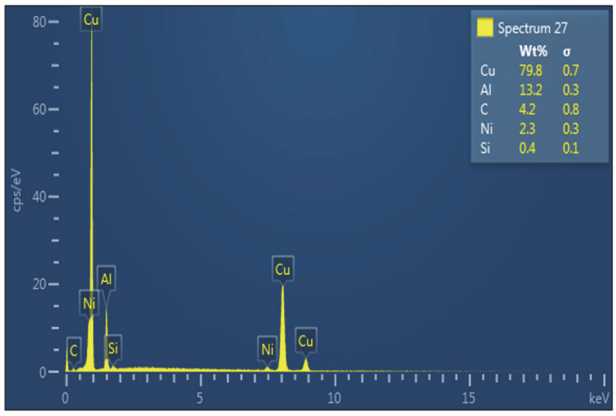

(b) EDX result for sample A Spectrum 27

Figure 6 Surface morphology and elemental compositions of 'Control' sample A

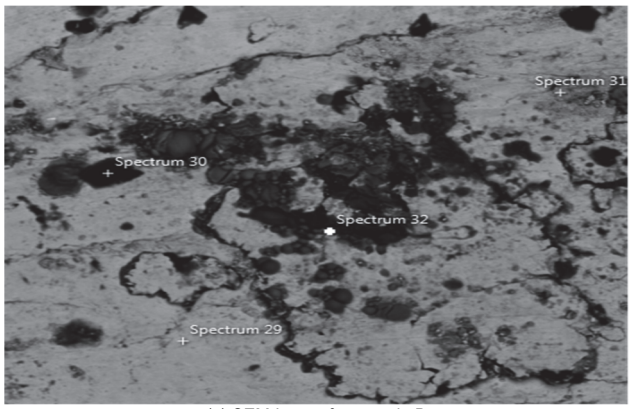

(a) SEM Image for sample B

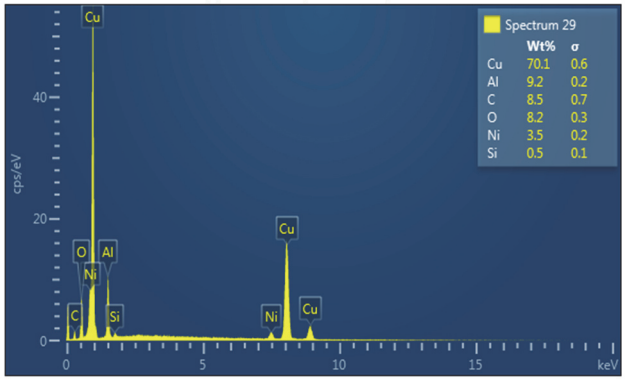

(b) EDX result for sample B Spectrum 29

Figure 7 Surface morphology and elemental compositions of Alloy sample B (SMA, 0.15% Graphene)

The identified debris in Fig. 6a have different shape and sizes which implies that the alloy solidified from melt to produce dendritic grains which grew at different rate until they intersect and interlock each other to assume the observed structures. Fig. 6b is the EDS (Energy Dispersive X-ray Spectroscope) result obtained to reveal the elemental analysis of the structure. It showed that micro-segregation occurs within the alloy due to different compositions of each element detected in the alloy from a point to another. At the point marked spectrum 27, the major elements detected are copper, aluminium, graphene (carbon) and nickel. Detection of silicon could be attributed to silica sand used in making the mould. The micrograph in Fig. 7, Fig. 8 and Fig. 9, presents the microstructure features of the graphene reinforced CuAlNiSMA.

Each of the microstructures shows an ash-like structure abhorring black-like or dark-like phases. It is observed in Fig. 7a representing CuAlNiSMA containing 0.15% graphene that the black phase sparsely distributes within the ash-like structure which is the host. Evidence of particle agglomeration is confirmed at the centre of the structure which contains crowded particle agglomerate. The black phase can be attributed to some compounds produced due to interactions of the graphene with any of the elements of the matrix or based alloy. This is evident from the result of the Energy Dispersive X-ray Spectroscope (EDS), Fig. 7b carried out showing the elemental compositions of the alloy.

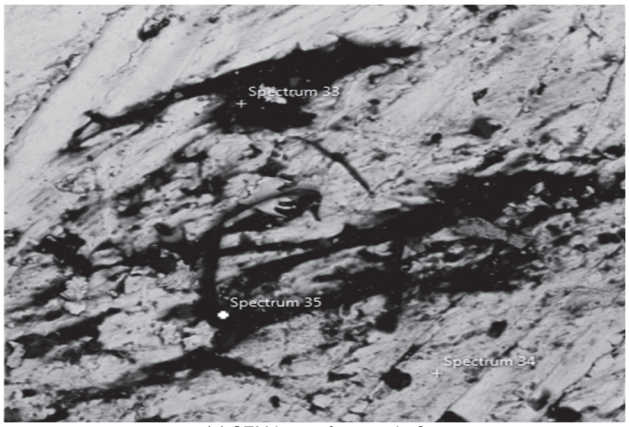

(a) SEM Image for sample C

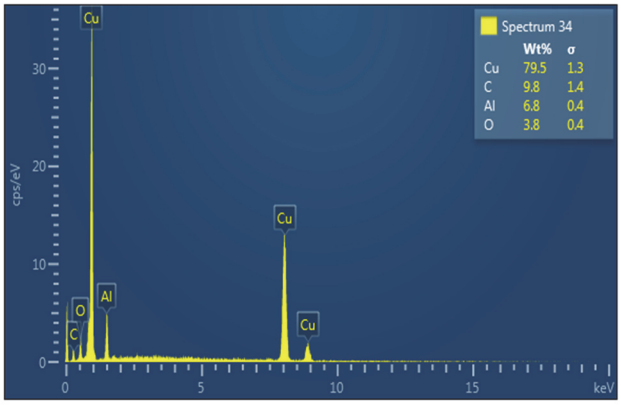

(b) EDX result for sample C Spectrum 34

Figure 8 Surface morphology and elemental compositions of Alloy sample C (SMA, 0.3% Graphene)

Fig. 8a above is the micrograph obtained for SMA containing 0.3% graphene. The microstructure shows clustered secondary black phase at different regions within

the structures. Moreover, the host structure has striations-like appearance which is joined together to form an undulating layer structures. Fig. 8b shows the EDS (Energy Dispersive X-ray Spectroscope) result obtained revealing the elemental compositions at spectrum 34. This confirmed the presence of copper based alloy. Nickel is not detected at this region probably because its concentration at this point is too low to be detected or the reflected x-ray from the nickel is marked or blocked by other detected elements.

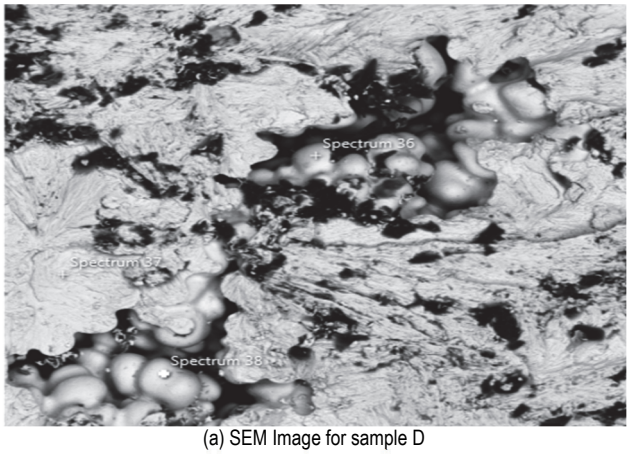

(a) SEM Image for sample D

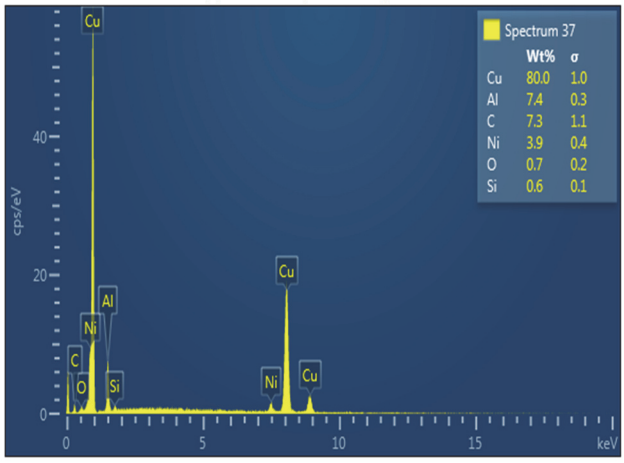

(b) EDX result for sample D Spectrum 37

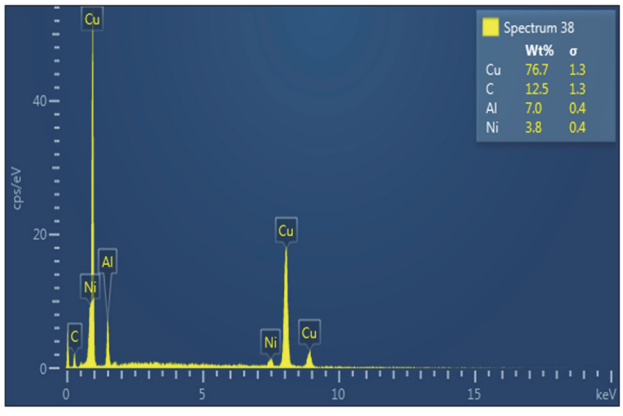

(b) EDX result for sample D Spectrum 38

Figure 9 Surface morphology and elemental compositions of Alloy sample D (SMA, 0.45% Graphene)

Fig. 9a is the micrograph of CuAlNiSMA containing 0.45% graphene. It is observed from the result that the host plain structure abhors rounded and black particles or grains existing as agglomerate. The plain structures appear as fortified egg strands. A fairly homogeneous structure is observed here, due to fairly even dispersions of the second phase particles. Fig. 9b and Fig. 9c shows the EDS (Energy Dispersive X-ray Spectroscope) results obtained revealing the elemental compositions at spectrum 37 and 38. The elemental compositions at different points affirmed that at different sections of the alloy it is very rich in copper which acts as the host for all other elements detected. Detection of silicon could be attributed to silica sand used in making the mould.

3.4.2 Effect of Graphene on Surface Morphologies and Properties of the Shape Memory Alloy

Comparing the SEM micrographs in Fig. 6 to Fig. 9 above, they show that Fig. 7, Fig. 8 and Fig. 9 SEM micrographs possess black particles which could be linked with compound precipitations due to interaction of the graphene which results in the formation of a new compound which has black colours. This is absent in Fig. 6 that has no graphene addition i.e. the control sample. The EDX result of Fig. 6b shows about 5% carbon is detected for sample A (control sample). This could be attributed to carbon pick-up from the ladle or crucible during the process of casting or inherent carbon in the alloy used as the matrix. Greater proportions of the carbon detected with the highest in the alloy containing 0.45% graphene (sample D) is linked with secondary black compound detected in each of the alloy reinforced with graphene, Fig. 7, Fig. 8 and Fig. 9. The secondary phase black particles in the host offer additional resistance to dislocation movement which causes greater dislocation hindrance or impingement. This requires additional stress for dislocation movement to cause indentations on the sample during the hardness measurement. Thus, this is responsible for the greater hardness values of each of the SMA containing graphene i.e. samples B, C and D as compared with sample A (control sample) without secondary black compound, Fig. 6. Highest number of cycles withstood by the alloy containing 0.3% graphene (sample C) during fatigue test could be attributed to fairly homogeneous structures of the alloy, Fig. 8. Fair dispersions of the carbon reduce the chances of local deformations that can cause fatigue failure at smaller number of cycles. This is observed in Fig. 9 for the alloy containing 0.45% graphene (sample D) that shows elements of discontinuity within the structure due to presence of rounded grains.

3.5 Data Analysis of Fatigue Life Using Analysis of Variance (ANOVA)

Two experimental parameters, namely the percentages of Cu and Graphene (C), were chosen as inputs for the experiment as shown in Tab. 5 for the analysis of variance (ANOVA). The output parameter in this case was the number of cycles to failure, which determines the fatigue life. As part of the experiment, a total of sixteen runs were conducted.

The summary of the model as shown from Tab. 6 above shows that the mathematical model for fatigue life indicates a good fit. Based on the model result, it means that the model can adequately predict the fatigue life given the R^2 (adj) = 0.9145.

Table 5 Input parameters and Output Responses

INPUT		OUTPUT
Graphene / %	Cu / %	Fatigue Life (cycles to failure) ($\times 10^3$)
0	84.3	1.7
0	84.78	1.2
0	84.05	0.7
0	83.92	0.5
0.15	84.3	1.5
0.15	84.78	1.1
0.15	84.05	0.6
0.15	83.92	0.3
0.3	84.3	1.8
0.3	84.78	1.0
0.3	84.05	0.7
0.3	83.92	0.5
0.45	84.3	0.9
0.45	84.78	0.7
0.45	84.05	0.4
0.45	83.92	0.2

Fatigue Life = 0.8625 + 0.1625 Graphene (%)
(0.00) + 0.0125 Graphene (%)
(0.15) + 0.1375 Graphene (%)
(0.30) – 0.3125 Graphene (%) (0.45)

Table 6 Model Summary

S	R^2	R^2 (adj)	PRESS	R^2 (pred)
0.142400	0.9487	0.9145	0.57679	0.8379

4 CONCLUSIONS

The addition of a small amount of high-purity graphene (C) nanoplatelets (0.3%) into CuAlNi SMA improves its fatigue life, with the optimum composition being 84.05 Cu - 11.32 Al - 3.79 Ni - 0.3 C wt. % (sample C) at 1649.25 MPA. The S-N curves show that higher stress cycles correspond with lower stress levels leading to fatigue failure. Microstructure analysis using SEM reveals that the presence of secondary black compounds linked with graphene contributes to increased hardness and mechanical properties. Design Expert Software version 13.0 was used to predict the interaction between Cu and graphene percentages with fatigue life, providing a novel and feasible mathematical model with an *R*-squared value of 0.9487. The model can be used to predict fatigue life for shape memory alloys containing graphene. SMA has many useful engineering applications such as in rice cooker, air conditioner for heating and cooling, coffee maker to mention but few. In the light of this, this research is very important to the field of engineering. It reveals the effect of graphene addition to the mechanical and fatigue behaviour of CuAlNi Shape Memory Alloy. A model was developed which can be deployed in study of fatigue life of SMA involving a quaternary element like graphene. The mathematical model developed for fatigue life has the merit of ease of access of the equation. This makes it easy to feel the impact of each of the input parameters on the fatigue life of the alloy. The developed model also provides a good framework to researchers in the area for further research.

5 REFERENCES

[1] Callister, W. D. & Rethwisch, D. G. (2018). *Materıals Science and Engineering An Introduction*. John Wiley & Sons, 10th ed. Inc.

[2] Ataalla, T., Leary, M., & Subic, A. (2012). Functional Fatigue of Shape Memory Alloys. *Sustainable Automotive Technologies 2012*, 39-43. https://doi.org/10.1007/978-3-642-24145-1_6

[3] Hartl, D. J. & Lagoudas, D. C. (2007). Aerospace applications of shape memory alloys. *Journal of Aerospace Engineering, 221*, 535-552. https://doi.org/10.1243/09544100JAERO211

[4] Petrini, L. & Migliavacca, F. (2011). Biomedical applications of shape memory alloys. *Journal of metallurgy,* 1-14 https://doi.org/10.1155/2011/501483

[5] Ma, J., Karaman, I., & Noebe, R. D. (2010). High temperature shape memory alloys. *International Materials Review, 55*, 257-315. https://doi.org/10.1179/095066010X12646898728363

[6] Tsuchiya, K. (2011). Mechanisms and properties of shape memory effect and superelasticity in alloys and other materials: A practical guide. *Shape Memory and Superelastic Alloys*, 3-14. https://doi.org/10.1533/9780857092625.1.3

[7] Kumar, P. K. & Lagoudas, D. C. (2008). *Introduction to Shape Memory Alloys*. Shape Memory Alloys Modelling and Engineering Applications. Springer. https://doi.org/10.1007/978-0-387-47685-8_1

[8] Saud, S. N., Hamzah, E., Abubakar, T. A., & Hosseinian, R. (2013). A Review on Influence of Alloying Elements on the Microstructure and Mechanical Properties of Cu-Al-Ni Shape Memory Alloys. *Jurnal Teknologi, 64*(1). https://doi.org/10.11113/jt.v64.1338

[9] Safaa Najah, S. A. (2019). *Cu-Based Shape Memory Alloys: Modified Structures and Their Related Properties*. Recent Advancements in the Metallurgical Engineering and Electrodeposition. https://doi.org/10.5772/intechopen.86193

[10] Al-Humairi, S. N. S. (2022). *Cu-based shape memory alloys: modified structures and their related properties*. Recent Advancements in the Metallurgical Engineering and Electrodeposition. https://doi.org/10.5772/intechopen.86193

[11] Jani, J. M., Leary, M., Subic, A., & Gibson, M. A. (2014). A review of shape memory alloy research, applications and opportunities. *Materials Design, 56*, 1078-1113 https://doi.org/10.1016/j.matdes.2013.11.084

[12] Prasad, K., Bazaka, O., Chua, M., Rochford, M., Fedrick, L., Spoor, J., Symes, R., Tieppo, M., Collins, C., Cao, A., Markwell, D., Ostrikov, K., & Bazaka, K. (2017). Metallic biomaterials: Current challenges and opportunities. *Materials, 10*(8), 884. https://doi.org/10.3390/ma10080884

[13] Canbay, C. A., Karaduman, O., & Özkul, İ. (2020). Lagging temperature problem in DTA/DSC measurement on investigation of NiTiSMA. *Material Science*: *Materials in Electronics, 31*(16), 13284-13291. https://doi.org/10.1007/s10854-020-03881-y

[14] Lojen, G., Anžel, I., Kneissl, A., Križman, A., Unterweger, E., Kosec, B., & Bizjak, M. (2015). Microstructure of rapidly solidified Cu–Al–Ni shape memory alloy ribbons. *Journal of Materials Processing Technology, 162-163*, 220-229. https://doi.org/10.1016/j.jmatprotec.2005.02.196

[15] López-Ferreño, I., Gómez-Cortés, J. F., Breczewski, T., Ruiz-Larrea, I., Nó, M. L., & San Juan, J. M. (2020). High-temperature shape memory alloys based on the Cu-Al-Ni system: design and thermomechanical characterization. *Journal of Materials. Research. & Technology, 9*(5), 9972- 9984. https://doi.org/10.1016/j.jmrt.2020.07.002

[16] Dasgupta, R. (2014). A look into Cu-based shape memory alloys: Present scenario and future prospects. *Journal of Materials Research*, *29*(16), 1681-1698. https://doi.org/10.1557/jmr.2014.189

[17] Issa, W. A., Camur, H., & Savas, M. (2021). A brief review of characteristics and applications of shape memory alloys in

engineering and related fields. *International Journal of Mechanical Engineering and Technology,12*(9), 34-43.
[18] Karaduman, O. & Canbay, C. A. (2021). Investigation of CuAlNi Shape Memory Alloy Doped with Graphene. *Journal of Materials & Electronic Devices, 3*, 8-14.
[19] Sellitto, A. & Riccio, A. (2019). Overview and future advanced engineering Applications for morphing surfaces by shape memory alloy materials. *Materials, 12*, 708. https://doi.org/10.3390/ma12050708
[20] Leal, P. B. & Savi, M. A. (2018). Shape memory alloy-based mechanism for aeronautical application: Theory, optimization and experiment. *Aerospace Science & Technology, 76*, 155-163. https://doi.org/10.1016/j.ast.2018.02.010
[21] Oliveira, J. P., Crispim, B., Zeng, Z., Omori, T., Braz Fernandes, F. M., & Miranda, R. M. (2019). Microstructure and mechanical properties of gas tungsten arc welded Cu-Al-Mn shape memory alloy rods. *Journal of Materials Processing Technology, 271*, 93-100. https://doi.org/10.1016/j.jmatprotec.2019.03.020
[22] Yang, S., Zhang, J., Chen, X., Chi, M., Wang, C., & Liu, X. (2019). Excellent superelasticity and fatigue resistance of Cu-Al-Mn-W shape memory single crystal obtained only through annealing polycrystalline cast alloy. *Journal of Materials Science. and Engineering, 749*, 249-254. https://doi.org/10.1016/j.msea.2019.02.033
[23] Tian, J., Zhu, W., Wei, Q, Wen, S., Li, S., Song, B., & Shi, Y. (2019). Process optimization, microstructures and mechanical properties of a Cubased shape memory alloy fabricated by selective laser melting. *Journal of Alloys and Compounds,785*, 754-764. https://doi.org/10.1016/j.jallcom.2019.01.153
[24] Vajpai, S. K., Dube, R. K., & Sangal, S. (2011). Microstructure and properties of Cu-Al-Ni shape memory alloy strips prepared via hot densification rolling of argon atomized powder preforms. *Materials Science & Engineering: A, 529*(1), 378-387. https://doi.org/10.1016/j.msea.2011.09.046
[25] Razooqi, R. N., Razej, K. H., Abdulhameed, A. T., & Irhayyim, S. S. (2018). The physical and mechanical properties of a shape memory alloy reinforced with carbon nanotubes (CNTs). *Tikrit Journal of Pure Science*, *23*(9), 80-88. https://doi.org/10.25130/tjps.v23i9.816
[26] Saud, S. N., Hamzah, E., Abu Bakar, T. A., & Abdolahi, A. (2014). Influence of addition of carbon nanotubes on structure–properties of Cu-Al-Ni shape memory alloys. *Materials Science & Engineering: A, 30*(4), 458-464. https://doi.org/10.1179/1743284713Y.0000000379
[27] Vanderson, M. D., Sergio, A. O., Marcelo, A. S., Pedro Manuel, C. P., & Luis Felipe, G. (2020). Fatigue on shape memory alloys: Experimental observations and constitutive modelling. *International Journal of Solids and Structures, 213*, 1-24. https://doi.org/10.1016/j.ijsolstr.2020.11.023
[28] Bhandari, V. D. (2016). *Design of machine elements*. MC GRAW HILL INDIA.
[29] Ugural, A. C. & Fenster, S. K. (2012). *Advanced Mechanics of Materials and Applied Elasticity*. Pearson Education, Inc.
[30] Obiukwu, O., Nwafor, M., & Grema, L. (2015). The effect of surface finish on the low cycle fatigue of low and medium carbon steel. *International Conference on Mechanical and Industrial Engineering (ICMIE 15)*,14-15.
[31] Savas, A. M. *Mechanical Properties of Composites Lecture Notes (MEE 571).* Near East University, Nicosia, Cyprus.
[32] XU, H., et al. (2008). A study on shape memory performance of single crystal Cu-Al-Ni-Be alloy. *Materials Review, 4*, 036.
[33] Xu, H. P., Song, G. F., & Mao, X., M. (2011). Influence of Be and Ni to Cu-Al alloy shape memory performance. *Advanced Materials Research, 197*, 1258-1262. https://doi.org/10.4028/www.scientific.net/AMR.197-198.1258
[34] Saud, S. N., Hamzah, E., Abubakar, T., Zamri, M., & Tanemura, M. (2014). Influence of Ti additions on the martensitic phase transformation and mechanical properties of Cu-Al-Ni shape memory alloys. *Journal of Thermal Analysis and Calorimetry, 118*, 111-122. https://doi.org/10.1007/s10973-014-3953-6
[35] Saud, S. N., Hamzah, E., Abu Bakar, T. A., & Abdolahi, A. (2014). Influence of addition of carbon nanotubes on structure-properties of Cu-Al-Ni shape memory alloys. *Journal of Materials Science and Technology*, *30*(4), 458-464. https://doi.org/10.1179/1743284713Y.0000000379

Contact information:

Wasiu Ayinde ISSA
(Corresponding author)
Kwara State University, Malete, Nigeria,
Department of mechanical engineering, KWASU, P. M. B. 1530, Ilorin, Nigeria
E-mail: 20195806@std.neu.edu.tr

Hüseyin ÇAMUR, Associate Professor
Near East University, Nicosia, Cyprus,
Department of Mechanical Engineering, Faculty of Engineering, 99138 Cyprus
E-mail: huseyin.camur@neu.edu.tr

Mahmut SAVAŞ, Professor
Near East University, Nicosia, Cyprus,
Department of Mechanical Engineering, Faculty of Engineering, 99138 Cyprus
E-mail: mahmut.savas@neu.edu.tr